Optimization of Block-cave Production Scheduling under Grade Uncertainty

Saha Malaki and Yashar Pourrahimian
Mining Optimization Laboratory (MOL)
University of Alberta, Edmonton, Canada

Abstract

The initial evaluation of a range of levels for starting the extraction of block-cave mining is an important issue. To do this, it is necessary to consider a variety of parameters including extraction rate, block height, discount rate, block profit, cost of mining and processing and revenue factors. Afterwards, production scheduling plays a key role in the entire project's profitability, determining the amount, grade and sequence of the extraction during the mine life by optimizing particular objectives in the presence of operational and technical constraints. To consider grade uncertainty, a set of simulated realizations of the mineral grade is modeled based on stochastic sequential simulation.

The purpose of this paper is to present a methodology to find the best extraction level and the optimum sequence of extraction for that level under grade uncertainty. Maximum net present value (NPV) is determined using a mixed-integer linear programming (MILP) model after choosing the best level of extraction given some constraints such as mining capacity, production grade, extraction rate and precedence. Application of the method for block-cave production scheduling using a case study over 15 Periods is presented.

1. Introduction

Among the underground mining methods available, caving methods are favored because of their low-cost and high-production rates. Production scheduling in block caving, because of its significant impact on the project's value, has been considered a key issue to be improved. To that end, researchers have applied different methods such as mathematical programming to model production scheduling in block caving. These models are built to help the decision-maker evaluate the consequences of various management alternatives. In order to be most useful, the decision support model should also include information about the uncertainties related to each of the decision options, as the certainty of the desired outcome may be central criterion on the selection of the management policy.

Ore-grade is one of the crucial parameters subject to uncertainty in mining operations. Grade uncertainty can lead to significant differences between actual production and planning expectations and, as a result, the net present value (NPV) of the project (Koushavand and Askari-Nasab, 2009,Osanloo et al., 2008). Various researchers have considered the effects of grade uncertainty in open-pit mines and introduced different methodologies to address those effects. Dowd (1994) presented a risk-based algorithm for surface mine planning. In the algorithm, for different variables such as commodity price, processing cost, mining cost, investment required, grade and tonnages, a predefined distribution function was implemented. Several types of schedules were generated for a number of realizations of the grades. This methodology produces various schedules that account for grade uncertainty. Ravenscroft (1992) and Koushavand and Askari-Nasab (2009) used simulated ore-bodies to show the influence of the grade uncertainty on production scheduling. Ramazan and Dimitrakopoulos (2004) used a mixed-integer linear programming (MILP) model to maximize the NPV for each realization. Then they calculated the probability of extraction of a block at each period. These probabilities are the input of a second stage of the optimization, which is necessary in order to generate one schedule at the end. Dimitrakopoulos and Ramazan (2008) presented a stochastic integer programming (SIP) model to generate optimal production schedules. This model considers multiple realizations of the block model and defines a penalty function that is the cost of deviation from the target production. This cost is calculated based on the geological risk discount rate which is the discounted unit cost of deviation from the target production. The objective function is to maximize the NPV under a managed risk profile. Leite and Dimitrakopoulos (2007) implemented an approach that incorporates the geological uncertainty in the open-pit mine scheduling process. This new scheduling approach is based on a simulated annealing (SA) technique and stochastically simulated representations of the ore-body. Albor and Dimitrakopoulos (2009) developed a method which is based on scheduling with an SA algorithm and equally probable realizations of a mineral deposit. To generate production schedules, the equally probable realizations are utilized to minimize the possibility of deviations from production targets. Sabour and Dimitrakopoulos (2011) presented a procedure that combines geological uncertainty and operational flexibility in the design of open-pits. When designing an optimal production schedule and ultimate pit limit, Asad and Dimitrakopoulos (2013) considered both geological uncertainty and commodity prices with respect to the production capacity restrictions. Two-stage stochastic integer programming (SIP) is used in an optimization model to consider uncertainty (Ramazan and Dimitrakopoulos, 2013). Lamghari and Dimitrakopoulos (2012) also considered metal uncertainty in the open-pit production scheduling problem using a metaheuristic solution approach based on a Tabu search. Lamghari et al. (2013) proposed two variants of a variable neighborhood decent algorithm to solve the open-pit mine production scheduling problem under geological uncertainty. Maleki and Emery (2015) have worked on the joint simulation of copper grade and rock type in a given deposit. To conduct the joint simulation, they implemented multi-Gaussian and pluri-Gaussian models in a combined form. They studied three main rock types with various grade distributions in which three auxiliary Gaussian random fields were considered. One of the rock types was used for copper grade simulation and the other two for rock-type simulation. Moreover, they looked at cross correlations between these Gaussian random fields before reproducing the dependence between copper grade and rock types.

Other than the aforementioned authors, few authors have examined geological uncertainty in underground mining. Grieco and Dimitrakopoulos (2007) implemented a new probabilistic mixed-integer programming model which optimizes the stope designs in sublevel caving. Vargas et al. (2014) developed a tool that considered geological uncertainty by using a set of conditional simulations of the mineral grades and defining the economic envelope in a massive underground mine. Montiel et al. (2015) incorporated geological uncertainty into their methodology that optimizes mining operation factors such as blending, processing, and transportation. They used a simulated annealing algorithm to deal with uncertainty. Carpentier et al. (2016) introduced an optimization formulation that looked at a group of underground mines under geological uncertainty. Their formulation evaluates the project's influence on economic parameters including capital investments and operational costs.

One of the main steps involved in optimizing underground mines is determining a mining outline and inventory. The open-pit corollary to this is open-pit optimization, which is completed with algorithms such as those by Lerchs and Grossmann (1965). To optimize block-caving scheduling, most researchers have used mathematical programming: linear programming (LP), MILP, and quadratic programming (QP). LP is the simplest program for modelling and solving. Table 1 shows some of the applied mathematical methodologies in block-caving production scheduling.

This paper will introduce a method designed to find the best level for initializing extraction according to the maximum discounted ore profit under grade uncertainty. Several realizations are modeled by using geostatistical studies to consider grade uncertainty. The production schedule is generated for the given advancement direction and in the presence of some constraints at the chosen level.

2. Methodology, assumption, and notations

The ore-body is represented by a geological block model. Numerical data are used to represent each block's attributes, such as tonnage, density, grade, rock type, elevation, and profit data.

The first step is to construct a block model based on the drillhole data and the grid definition. The next step is a geostatistical study to generate the realizations. Then, the best level of extraction is found. Finally, the optimal sequence of extraction is determined to maximize the NPV for each realization. Fig 1 shows the summary of the methodology.

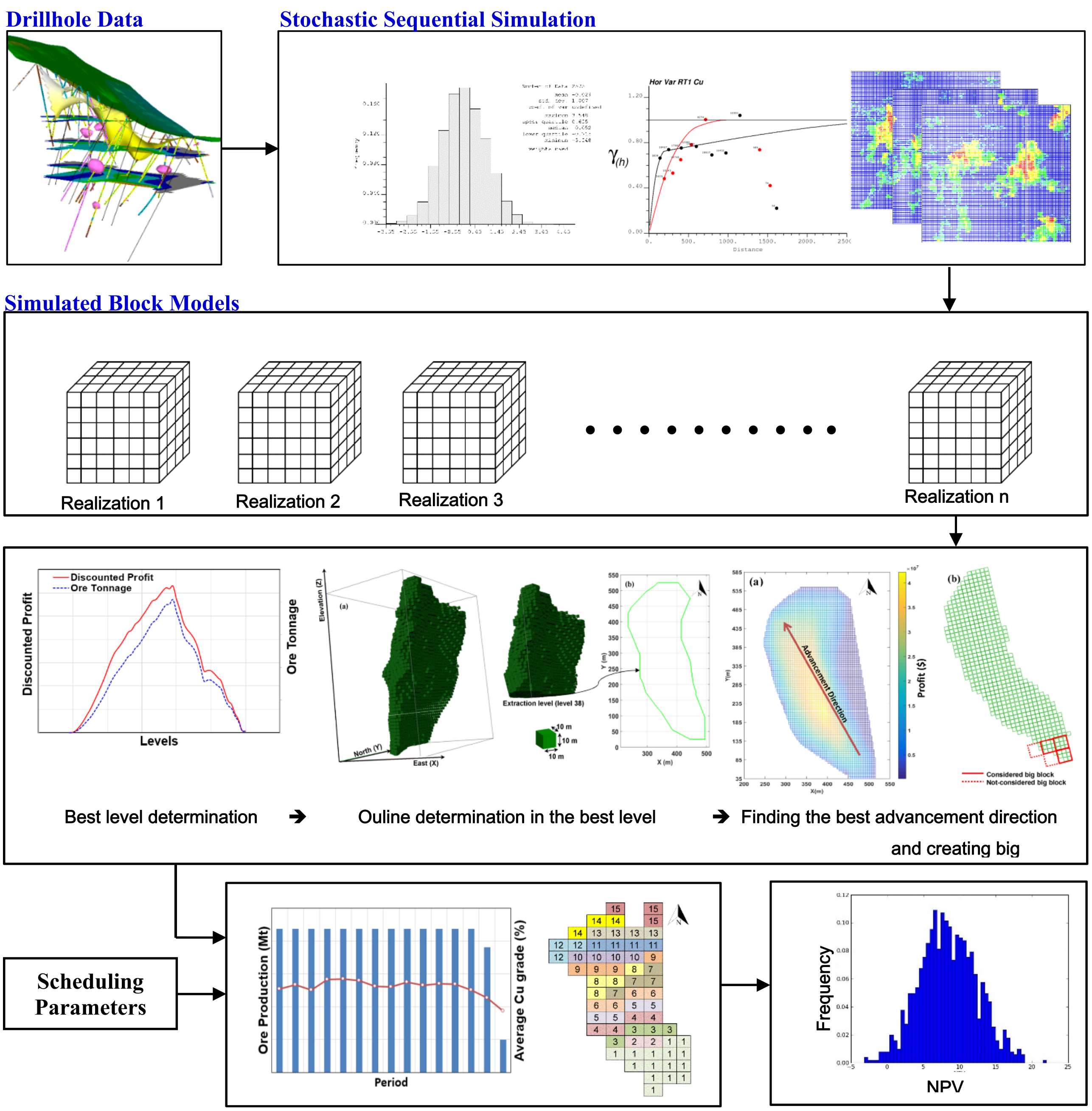

Fig 1. Steps of the implemented methodology

Table 1. Summary of applied mathematical methodologies in block-caving production scheduling (Khodayari and Pourrahimian, 2014)

<table>
<tr><th>Author</th><th>Methodology</th><th>Model's objective(s)</th><th>Features</th></tr>
<tr><td>Song (1989)</td><td>MILP</td><td>Minimization of total mining cost</td><td rowspan="14">LP

This method has been used most extensively and it can provide a mathematically provable optimum schedule. But straight LP lacks the flexibility to directly model complex underground operations which require integer decision variables.

MILP

MILP could be used to provide a series of schedules which are marginally inferior to a provable optimum. Computational ease in solving an integer-programming problem depends on the formulation structure. It can provide a mathematically provable optimum schedule. The advantage that MILP has over simulation when used to generate sub-optimal schedules is that the gap between the MILP feasible solution and the relaxed LP solution provides a measure of solution quality. The drawback in using MILP is that it is often difficult to optimize large production systems by the branch-and-bound search method.

QP

The block caving process is non-linear, so it would not be appropriate to use linear programming for production scheduling. But solving this kind of problem could be a challenge because we must change the formulation to LP and then solve the problem. Changing creates conversion errors.</td></tr>
<tr><td>Chanda (1990)</td><td>Simulation and MIP</td><td>Minimization of the deviation in the average production grade between operating shifts</td></tr>
<tr><td>Guest et al. (2000)</td><td>LP</td><td>Maximization of NPV</td></tr>
<tr><td>Rubio (2002)</td><td>MIP</td><td>Two models: (a) maximization of NPV and (b) optimization of the mine life</td></tr>
<tr><td>Diering (2004)</td><td>NLP</td><td>Maximizing NPV for M periods and minimization of the deviation between a current draw profile and a defined target</td></tr>
<tr><td>Rubio and Diering (2004)</td><td>LP, IP, QP</td><td>Maximization of NPV, optimization of draw profile, and minimization of the gap between long- and short-term planning</td></tr>
<tr><td>Rahal et al. (2008)</td><td>MILGP</td><td>Minimizing deviation from the ideal draw profile while achieving a production target</td></tr>
<tr><td>Weintraub et al. (2008)</td><td>MIP</td><td>Maximization of profit</td></tr>
<tr><td>Smoljanovic et al. (2011)</td><td>MILP</td><td>Optimization of NPV and mining material handling system</td></tr>
<tr><td>Parkinson (2012)</td><td>IP</td><td>Finding an optimal opening sequence in an automated manner</td></tr>
<tr><td>Epstein et al. (2012)</td><td>LP, IP</td><td>Maximization of NPV</td></tr>
<tr><td>Diering (2012)</td><td>QP</td><td>Objective tonnage (to optimize the shape of the cave)</td></tr>
<tr><td>Pourrahimian et al. (2013)</td><td>MILP</td><td>Maximization of NPV</td></tr>
<tr><td>Alonso-Ayuso et al. (2014)</td><td>MILP</td><td>Maximization of NPV taking into consideration the uncertainty in copper price</td></tr>
<tr><td>Pourrahimian and Askari-Nasab (2014)</td><td>MILP</td><td>Maximization of NPV, determining the BHOD based on the optimization</td><td></td></tr>
</table>

2.1. Geological uncertainty

The first step for a geostatistical study is to define different rock types based on the drillhole data. In this study, which assumes a stationary domain within each rock type, the geostatistical modeling is performed for each rock type separately. The following steps are common for generating a geological model:

First, a declustering algorithm is used to get the representative distribution of each rock type to decrease the weight of clustered samples. Then, the correlation of the multivariate data is determined. To determine the principle directions of continuity, global kriging is performed using arbitrary variograms with a high range. Indicator kriging is used for rock type modeling, and simple kriging is used for grade modeling. The data is transformed to Gaussian units to remove the correlation between the variables in each rock type.

The experimental variograms are calculated by using the determined directions of continuity in the previous step and a model is fitted to these variograms in different directions. An indicator variogram is used for rock type modeling and a traditional variogram is used for grade modeling. A rock type model is generated for the chosen grid definition by using a sequential indicator simulation algorithm (SIS). A grade model for each rock type is generated based on a Sequential Gaussian Simulation algorithm (SGS). Then, the data is back-transformed to original units. Finally, grade modeling is done within each rock type.

2.2. Placement of extraction level

To find the best level of extraction, the ore tonnage and discounted profit are calculated for each level of the block model. The discounted profit of each ore block (Diering et al., 2008) and the total discounted profit of each level are calculated using equations. (1) and (2).

$$Dis\ \mathrm{P}_{blL} = \sum_{l=L}^{1} \frac{\mathrm{Pr}_{bll}}{(1+i)^{d/ER}}, \quad \forall bl \tag{1}$$

$$Dis\ \mathrm{P}_{L} = \sum_{bl=1}^{BL} Dis\ \mathrm{P}_{blL} \tag{2}$$

Where $Dis\ \mathrm{P}_{blL}$ is the discounted profit of ore block bl at level L; $Dis\ \mathrm{P}_{L}$ is the total discounted profit of level L, which is the summation of discounted profit of all the blocks in that level; Pr_{bll} is the profit (undiscounted) of ore block bl at level l; i is the discount rate; d is the distance between the center points of ore block bl at level L and the ore blocks above it; ER is the extraction rate per period; BL is the total number of ore blocks in level L. The profit of each ore block is calculated using the following equations:

$$T_R = g \times Ton \times R \times (P - S_C) \tag{3}$$

$$T_C = Ton \times (M_C + P_C) \tag{4}$$

$$P = T_R - T_C \tag{5}$$

Where T_R is the total revenue; R is the processing plant recovery; P is the price per ton of the product; S_C is the selling cost per ton of material; g is the element grade; T_C is the total cost; P_C is the processing plant cost and M_C is the cost of mining per ton of material. Fig 2 clearly shows how to calculate the discounted profit of a block at a given level. In Fig 2, two blocks are assumed to be in each level. Afterwards, the tonnage-profit curve is plotted and the level with the highest profit is selected for starting the extraction (Fig 3).

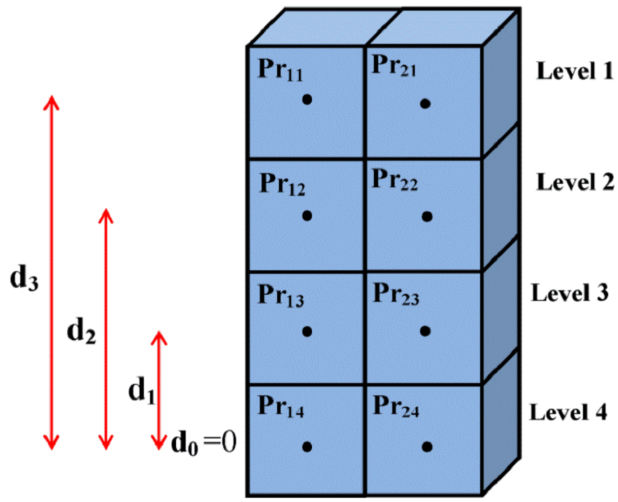

$$Dis\ \mathrm{P}_{14} = \frac{\mathrm{Pr}_{14}}{(1+i)^{d_0/ER}} + \frac{\mathrm{Pr}_{13}}{(1+i)^{d_1/ER}} + \frac{\mathrm{Pr}_{12}}{(1+i)^{d_2/ER}} + \frac{\mathrm{Pr}_{11}}{(1+i)^{d_3/ER}}$$

$$Dis\ \mathrm{P}_{24} = \frac{\mathrm{Pr}_{24}}{(1+i)^{d_0/ER}} + \frac{\mathrm{Pr}_{23}}{(1+i)^{d_1/ER}} + \frac{\mathrm{Pr}_{22}}{(1+i)^{d_2/ER}} + \frac{\mathrm{Pr}_{21}}{(1+i)^{d_3/ER}}$$

$$Dis\ \mathrm{P}_{Level4} = Dis\ \mathrm{P}_{14} + Dis\ \mathrm{P}_{24}$$

Fig 2. Schematic example of calculating discounted profit of ore block at a given level

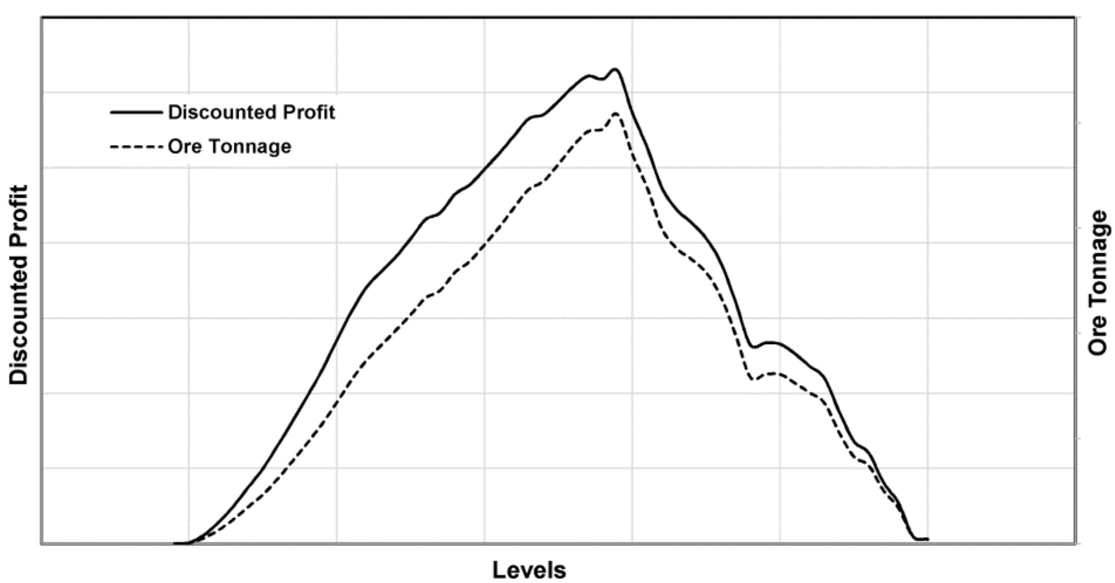

Fig 3. Schematic view of finding best level of extraction methodology

2.3. Production scheduling

After determining the best elevation, the interior of the ore-body outline in the level is divided into rectangles based on the minimum required mining footprint (see Fig 4). The minimum mining footprint (plan view) represents the minimum sized shape that will induce and sustain caving. This is similar to the hydraulic radius in a caving operation. Then all block inside of the rectangle and above that creates big-blocks. In the next step, the sequence of extraction of these big-blocks is optimized.

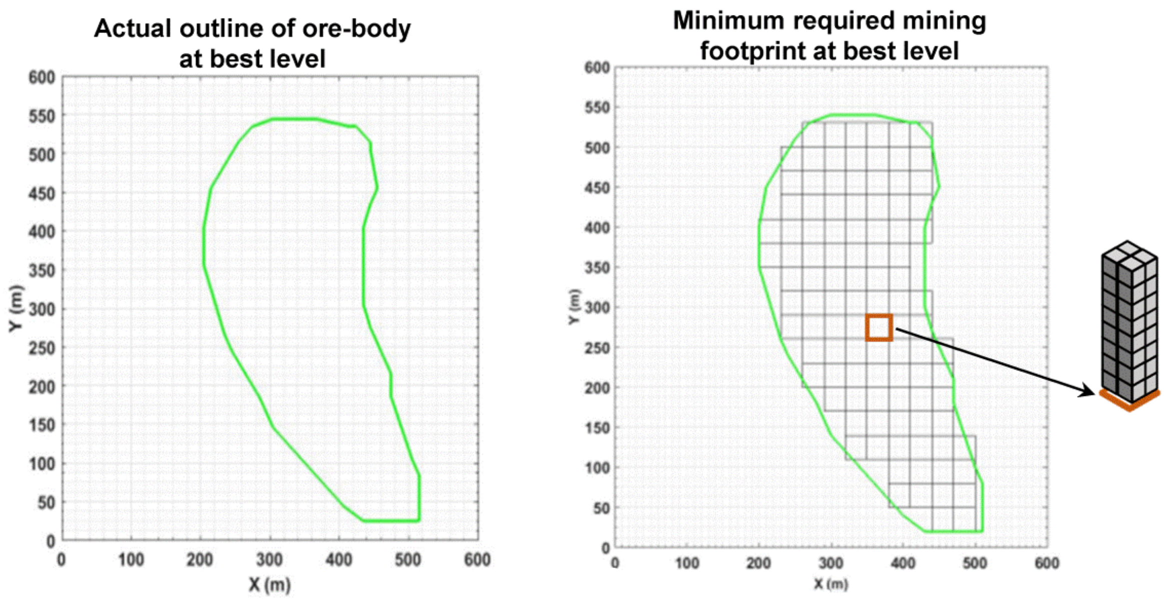

Fig 4. Schematic view of production scheduling methodology

3. Mathematical formulation

3.1. Notation

The notation of sets, indices and decision variables for the MILP model are as follows:

Indices

$t \in \{1,....,T\}$ Index for scheduling periods.

$bl \in \{1,...,BL\}$ Index for small blocks.

$bbl \in \{1,...,BBL\}$ Index for big-blocks.

Set

S^{bbl} For each big-block, bbl , there is a set S^{bbl} , which define the predecessor big-blocks that must be started prior to extracting the big-block bbl .

Decision variables

$B_{bbl,t} \in \{0,1\}$ Binary variable controlling the precedence of the extraction of big-blocks. It is equal to one if the extraction of big-block bbl has started by or in period

t ; otherwise it is zero.

$x_{bbl,t} \in [0,1]$	Continuous variable, representing the portion of big-block bbl to be extracted in period t .
$y_{bbl,t} \in \{0,1\}$	Binary variable used for activating either of two constraints.

Parameters

$Profit_{bbl}$	Profit of each big-block.
Ton_{bbl}	Tonnage of each big-block.
$MCL\,(Mt)$	Lower bound of mining capacity.
$MCU\,(Mt)$	Upper bound of mining capacity.
g_{bbl}	Average grade of the element to be studied in big-block bbl
$GL\,(\%)$	Lower bound of acceptable average head grade of considered element.
$GU\,(\%)$	Upper bound of acceptable average head grade of considered element.
$ExtU\,(Mt)$	Maximum possible extraction rate from each big-block.
$ExtL\,(Mt)$	Minimum possible extraction rate from each big-block.
L	Arbitrary big number.
T	Maximum number of scheduling periods.
BBL	Number of ore big-blocks in the model.
n	Number of predecessor big-blocks of big-block bbl
$\overline{N}_{NBBL,t}$	Upper bound for the number of new big-blocks, the extraction from which can start in period t
$\underline{N}_{NBBL,t}$	Lower bound for the number of new big-blocks, the extraction from which can start in period t

3.2. Objective function and constraints

The objective function of the MILP formulation is to maximize the NPV of the mining operation, which depends on the value of the big-blocks. (Based on distances between drawpoints and footprint size, the ore blocks are placed into bigger blocks). The objective function, equation (6), is composed of the big-blocks' profit value, discount rate, and a continuous decision variable that indicates the portion of a big-block, which is extracted in each period. The most profitable big-blocks will be chosen to be part of the production in order to maximize the NPV.

$$Max \quad \sum_{t=1}^{T} \sum_{bbl=1}^{BBL} \frac{Profit_{bbl} \times x_{bbl,t}}{(1+i)^{t}} \tag{6}$$

Where $Profit_{bbl}$ is the profit value of the big-block bbl which is equal to the summation of the small ore blocks' profit within that big-block. The objective function is subject to the following constraints:

Mining capacity

$$MCL_t \le \sum_{bbl=1}^{BBL} Ton_{bbl} \times x_{bbl,t} \le MCU_t, \quad \forall t \in \{1,....,T\} \tag{7}$$

These constraints ensure that the total tonnage of material extracted from each big-block in each period is within the acceptable range. The constraints are controlled by the continuous variables.

Grade blending

$$GL_t \le \frac{\sum_{bbl=1}^{BBL} g_{bbl} \times Ton_{bbl} \times x_{bbl,t}}{\sum_{bbl=1}^{BBL} Ton_{bbl} \times x_{bbl,t}} \le GU_t, \quad \forall t \in \{1,...,T\} \tag{8}$$

These constraints ensure that the production's average grade is in the acceptable range.

Block extraction rate and continuous extraction constraints

$$Ton_{bbl} \times x_{bbl,t} \le ExtU_{bbl,t}, \quad \forall bbl \in \{1,...,BBL\}, t \in \{1,...,T\} \tag{9}$$

$$(ExtL_{bbl,t} \times B_{bbl,t}) - (Ton_{bbl} \times x_{bbl,t}) \le L \times y_{bbl,t}, \quad \forall bbl \in \{1,...,BBL\}, t \in \{1,...,T\} \tag{10}$$

$$\sum_{t'=1}^{t} x_{bbl,t'} \ge y_{bbl,t}, \quad \forall bbl \in \{1,...,BBL\}, t \in \{1,...,T\} \tag{11}$$

Equation (9) ensures that the extraction rate from each big-block per period does not exceed the maximum extraction rate. $y_{bbl,t}$ in equations (10) and (11) is a binary variable which is used to activate either equation (10) or (11). Whenever equation (10) is active, it ensures that minimum extraction rate from each big-block per period is extracted. If the remaining tonnage of a big-block is less than the minimum extraction rate, equation (11) will be activated and forces that big-block to be extracted as much as the remaining tonnage which results in continuous extraction from each big-block.

Binary constraints

$$x_{bbl,t} \le B_{bbl,t}, \quad \forall bbl \in \{1,...,BBL\}, \ t \in \{1,...,T\} \tag{12}$$

$$B_{bbl,t} - B_{bbl,t+1} \le 0, \quad \forall bbl \in \{1,...,BBL\}, \ t \in \{1,...,T\} \tag{13}$$

Equation (12) ensures that if the extraction of one big-block is started its binary variable should be one. Also equation (13) controls the fact that if the extraction of one big-block in period t has been started ($B_{bbl,t} = 1$), the related binary variable should be kept one till end of the mine life. Both equations (11) and (13) contribute to the continuity of the extraction. The results of these constraints will be used for the precedence constraint for which the maximum number of active big-blocks is needed.

Number of new big-blocks constraints

$$\underline{N}_{NBBL,1} \le \sum_{bbl=1}^{BBL} B_{bbl,1} \le \overline{N}_{NBBL,1} \ , \quad t=1 \tag{14}$$

$$\underline{N}_{NBBL,t} \le \sum_{bbl=1}^{BBL} B_{bbl,t} - \sum_{bbl=1}^{BBL} B_{bbl,t-1} \le \overline{N}_{NBBL,t} \quad , \ \forall t \in \{2,...,T\} \tag{15}$$

These two constraints ensure that the number of new big-blocks in each period should be in an acceptable range. It is obvious that the number of new drawpoints in period one is more than other periods; therefore equation (14) is applied to period one and equation (15) is applied from period two to the end of the mine life.

Precedence constraints

$$n \times B_{bbl,t} \le \sum_{k=0}^{n} B_{S^{bbl}(k),t} \quad , \quad \forall bbl \in \{1,...,BBL\}, \ t \in \{1,...,T\} \tag{16}$$

These constraints ensure that all the predecessor big-blocks of a given big-block bbl have been started prior to extracting this big-block.

To apply this constraint, first the adjacent big-blocks of each big-block are determined and then an advancement direction is defined. Afterwards, a perpendicular line to the advancement direction is imagined at the center point of the considered big-block. Then we have to find a point on the perpendicular line using equation (17). The coordinate of this point is (X_{new}, Y_{new}).

$$Y_{new} - y_{bbl} = -\frac{1}{m}(X_{new} - x_{bbl}) \tag{17}$$

Where m is the slope of the advancement direction; y_{bbl} and x_{bbl} are the coordinates of the considered big-block in the extraction level; X_{new} is an arbitrary coordinate and as a result, Y_{new} is calculated by equation (17). Then, using equation (18), the value of D is calculated for each adjacent big-block.

$$D = (x_{adj} - x_{bbl})(Y_{new} - y_{bbl}) - (y_{adj} - y_{bbl})(X_{new} - x_{bbl}) \tag{18}$$

Where x_{adj} and y_{adj} are the coordinates of the adjacent big-blocks of each big-block. By calculating D, if the mining direction points to the direction that y increases, big-blocks with $D<0$ are below the perpendicular line and considered as the predecessors of a given big-block and if not, big-blocks with $D>0$ are considered as predecessors of the specified big-block. The following example contributes significantly to a clear understanding of the methodology used for precedence constraint.

Fig 5 shows how to select the predecessors for different advancement directions. A big-block (red block) is considered and its adjacent big-blocks are BL1-BL8. In Fig 5, the blue arrow shows the advancement direction and the orange line is the imaginary perpendicular line at the center of the considered big-block. The related calculation has been summarized in Table 2. According to Fig 5a, the advancement direction is from SW to NE which means y is increasing; therefore the extraction of the big-blocks with the negative value of D should be started before the considered block. Fig 5b and Fig 5c are examples of positive values with similar directions. Big-blocks 4, 6, 7, and 8 and 6, 7, and 8 are predecessor big-blocks for red block in Fig 5b and Fig 5c respectively, as they have positive D . Also, in Fig 5d, as the advancement direction is from E to W and D should be negative, big-blocks 3, 5, and 8 that have negative D are chosen as the predecessors.

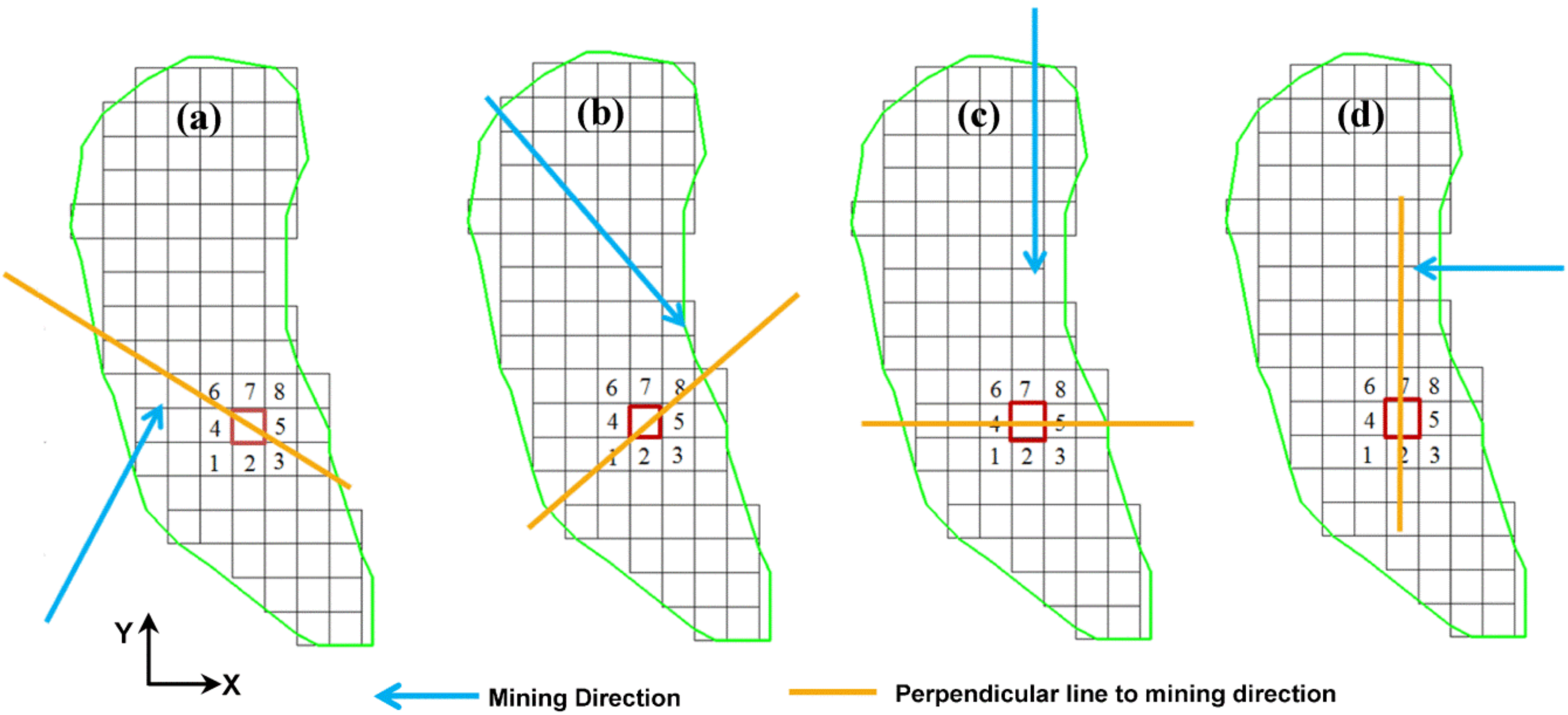

Fig 5. Schematic examples of methodology used in precedence constraint

Table 2. Example of calculation to find the predecessors of a big-block in the considered advancement direction (Fig 5a)

Direction: SW → NE
Slope of advancement direction: m = 1.8

Considered block's coordinates: (395,215)
$X_{new} = 200$

Adjacent blocks	1	2	3	4	5	6	7	8
Coordinates	(365,185)	(395,185)	(425,185)	(365,215)	(425,215)	(365,245)	(395,245)	(425,245)
D (Eq. (18))	< 0	< 0	< 0	< 0	> 0	> 0	> 0	> 0
predecessor	Yes	Yes	Yes	Yes	No	No	No	No

Reserve constraints

$$\sum_{t=1}^{T} x_{bbl,t} = 1, \quad \forall bbl \in \{1,...,BBL\} \tag{19}$$

In this formulation, all material inside of the big-blocks should be extracted. This is controlled by equation (19).

4. Solving the optimization problem

The proposed MILP model has been developed in MATLAB (Math Works Inc., 2015), and solved in the IBM ILOG CPLEX environment (IBM, 2015). A branch-and-bound algorithm is used to solve the MILP model, assuring an optimal solution if the algorithm is run to completion. Authors have used the gap tolerance (EPGAP) of 1% as an optimization termination criterion. This is an absolute tolerance between the gap of the best integer objective and the objective of the remained best node.

5. Case study

5.1. Grade uncertainty

A geostatistical study based on the drillhole data of a copper deposit and according to what is mentioned in section 2.1 was performed. Geostatistical software library (GSLIB) (Deutsch and Journel, 1998) was used for geostatistical modeling in this paper. The data belongs to the copper grade, so it is univariate data; this means there is no need for multivariate statistical analysis and transferring data to multivariate Gaussian framework to find the correlation between the variables. The initial inspection of the locations of the drillholes showed that the drillholes were equally spaced. As a result, the declustering algorithm was not implemented.

There were two parts to the modeling: rock type modeling and grade modeling. The grade modeling was implemented for both rock types (ore and waste) separately.

5.1.1. Rock type modeling

The principal directions of continuity were found using indicator kriging. Afterwards, the indicator variograms were calculated and a theoretical variogram model was fitted with three structures. In Fig 6 top left shows the plan view of maximum direction of continuity for rock types at Elevation 40 and experimental directional variograms (dots) and the fitted variogram models (solid lines) for rock type and distance units in meters. At the next step, 20 realizations for rock types were generated using an SIS algorithm. Plan view of rock type simulation for first realization at Elevation 40 is shown in Fig 6 (top right).

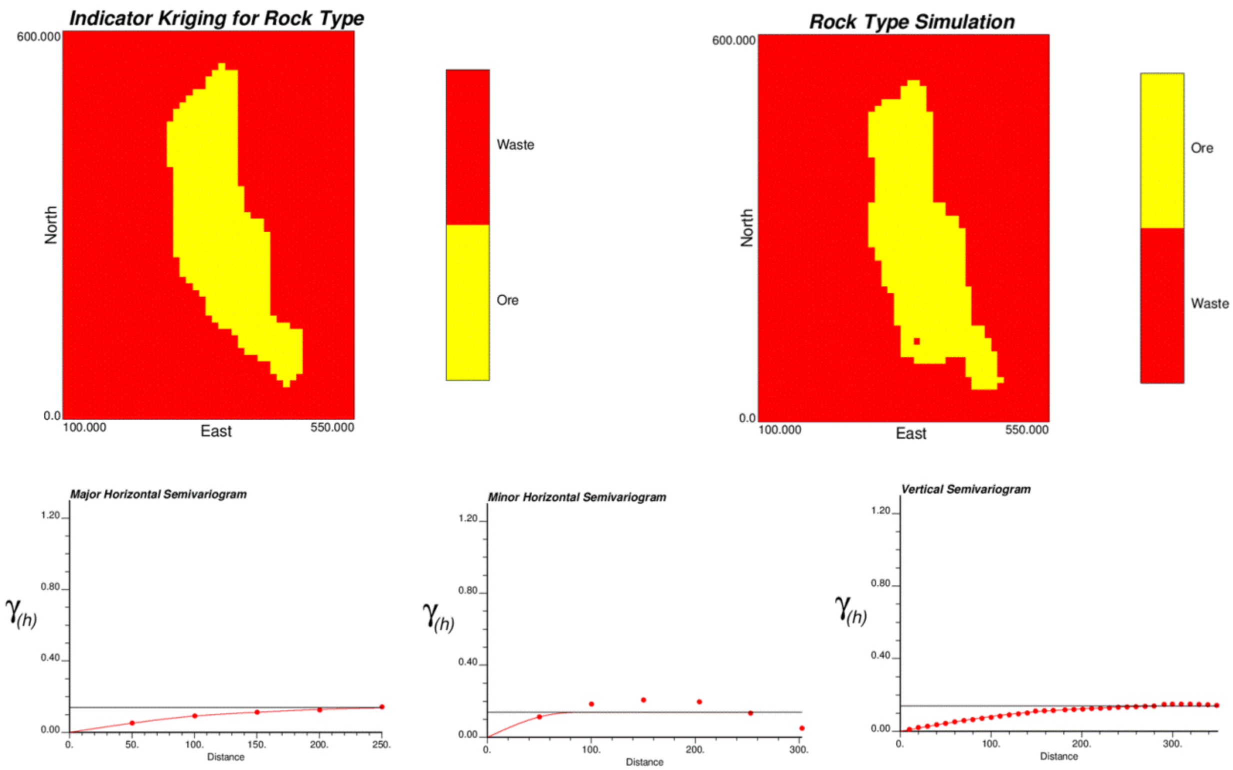

Fig 6. Rock type modeling and simulation

5.1.2. Grade Modeling

For ore modeling, the principal directions of continuity were extracted by doing simple kriging with the help of arbitrary variograms. Then the copper grades were transformed to Gaussian space. In Fig 7 top left shows plan view of maximum direction of continuity for copper grade at Elevation 40. Traditional variogram calculation and modeling with three structures and a nugget effect of 0.1 were done for the copper grade. Afterwards, 20 realizations for the copper grade were generated using SGS algorithms. The SGS needs a back-transformation to original units. The plan view of copper grade simulation for first realization at Elevation 40 is shown in Fig 7 top right.

5.1.3. Merging grade models into rock type models

The next step was to match and merge the rock type model with the grade model for each realization. Fig 8 shows the plan view of the final simulation for the first realization. Fig 9 shows the variogram reproduction of the rock-property (ore) simulation (top) and rock-type simulation (bottom) in three major, minor, and vertical directions. Since the variograms were reproduced quite reasonably, the generated realizations were considered representative of the grade uncertainty.

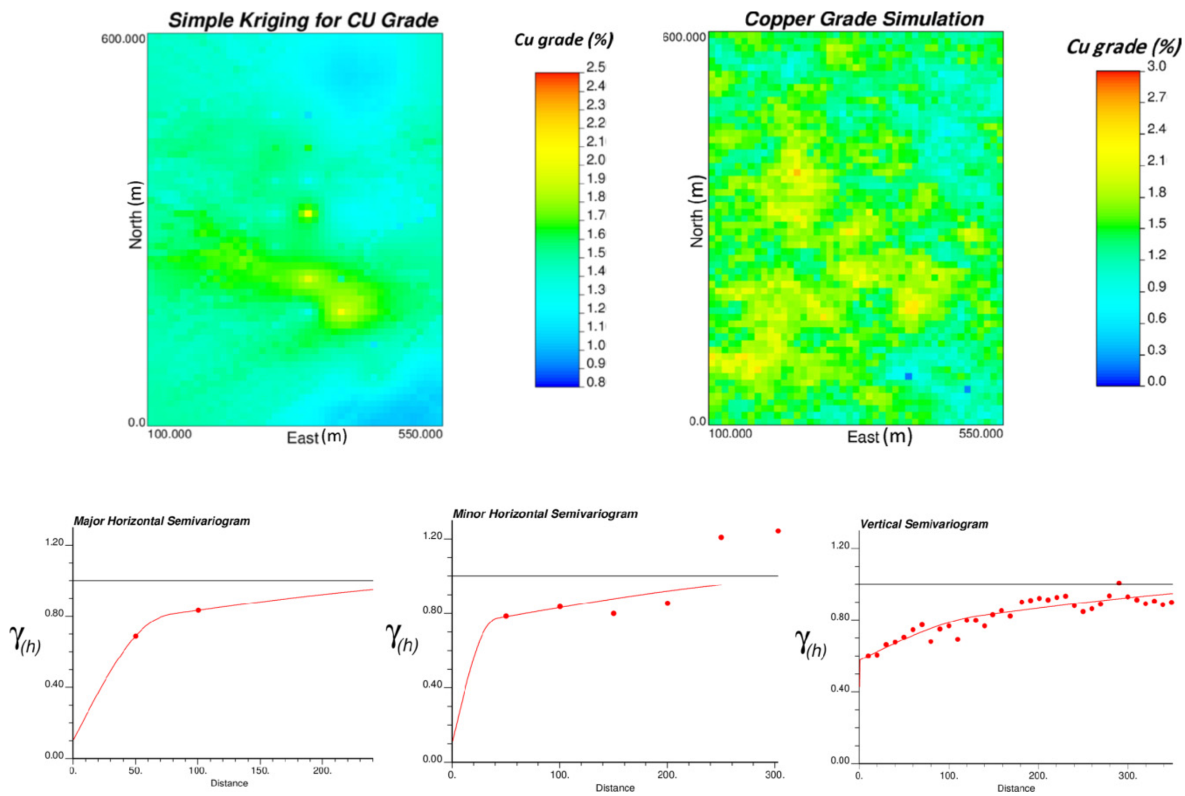

Fig 7. Grade modeling and simulation

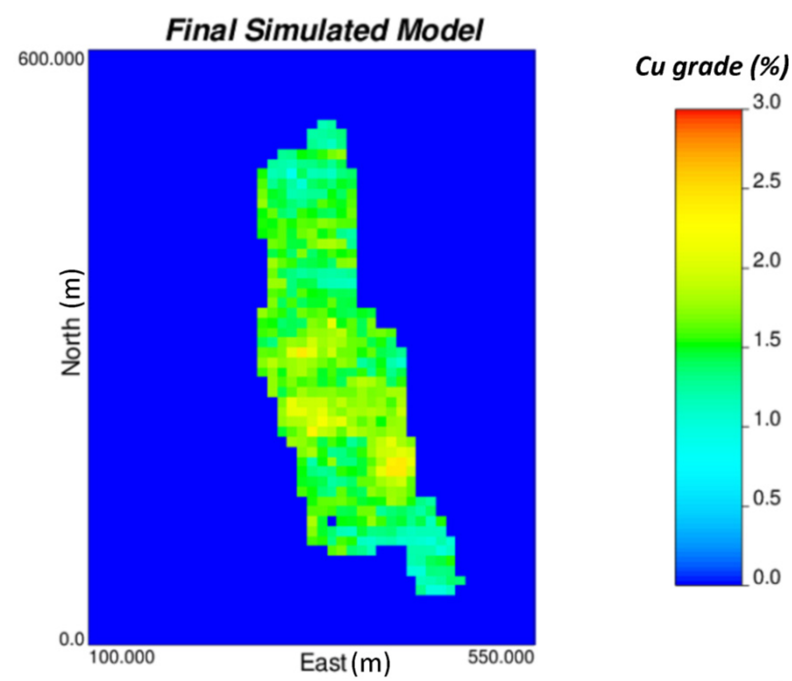

Fig 8. Final simulation of first realization at Elevation 40

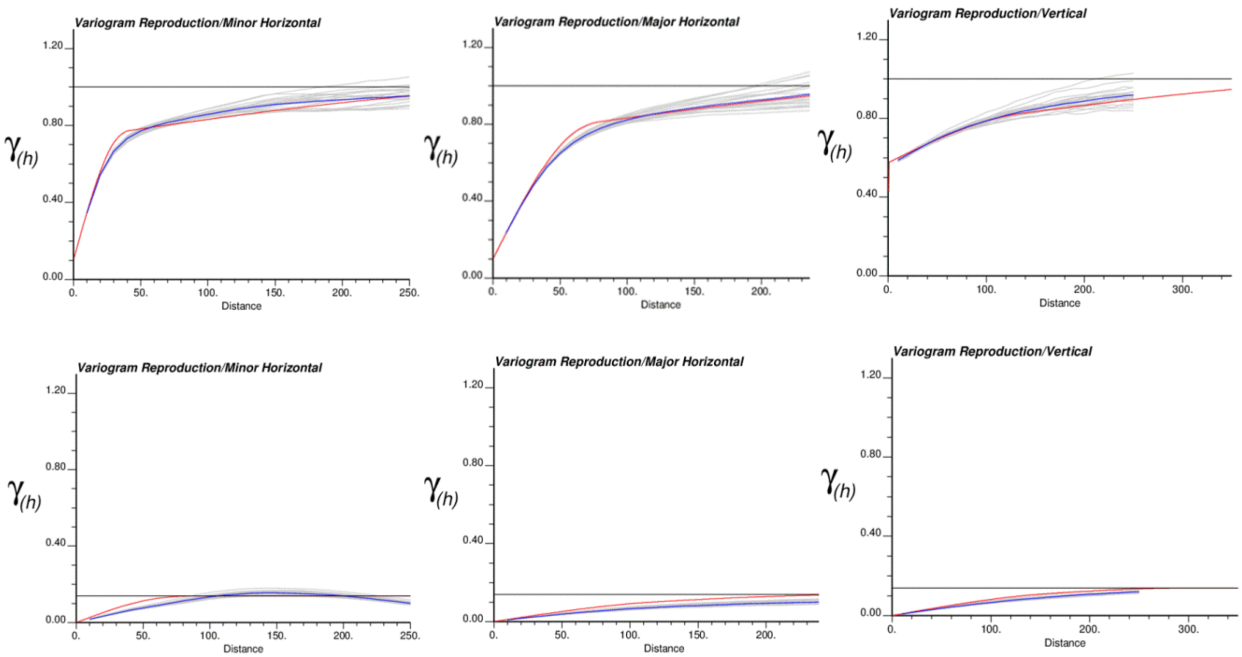

Fig 9. Variogram reproduction at Gaussian units of copper grade (top) and rock-type (bottom) realizations (gray lines), the reference variogram model (red line), and the average variogram from realizations (blue line) in three directions.

5.2. Placement of extraction level

The discounted profit and tonnage of the ore blocks above each ore block in each level were calculated and the profit-tonnage curve was plotted. The input parameters for calculating discounted profit as mentioned in section 2.2 are block height and extraction rate which were assumed to be 10 meters and 15 (meter/period) respectively. This led to selecting the best level for starting extraction based on maximum profit for each realization.

Fig 10a and 10b illustrate the best level of extraction for average simulated and original block models, respectively. Fig 10c shows the histogram of the obtained extraction levels for realizations, in 40 % of the realizations, level 39 is the best level of extraction.

To investigate the effect of the grade uncertainty, the presented MILP model should be applied on all the simulated block models. Then the NPVs of all simulated- , average simulated-, and original block model are compared. To create the average-simulated block model, the average grade of all the block models for each cell was calculated to consider one block model instead of all the block models and then the best level of extraction was found for the created average block model.

5.3. Production Scheduling

To maximize the NPV, the proposed mathematical model was applied to generate the production schedule for the level 39 of the all block models.

The ore blocks layout for level 39 was determined (e.g.Fig 11b). Then based on the method presented by Khodayari and Pourrahimian (2015) the best advancement direction for level 39 was determined (see Fig 12a) . Afterwards, because of the distances between drawpoints and the assumed footprint size (30m × 30m), the blocks were placed into bigger blocks along the advancement direction. Additionally, as the big-blocks close to the boundaries did not constitute a complete set (with nine small blocks), only sets with seven or more blocks were considered (see Fig 12b).

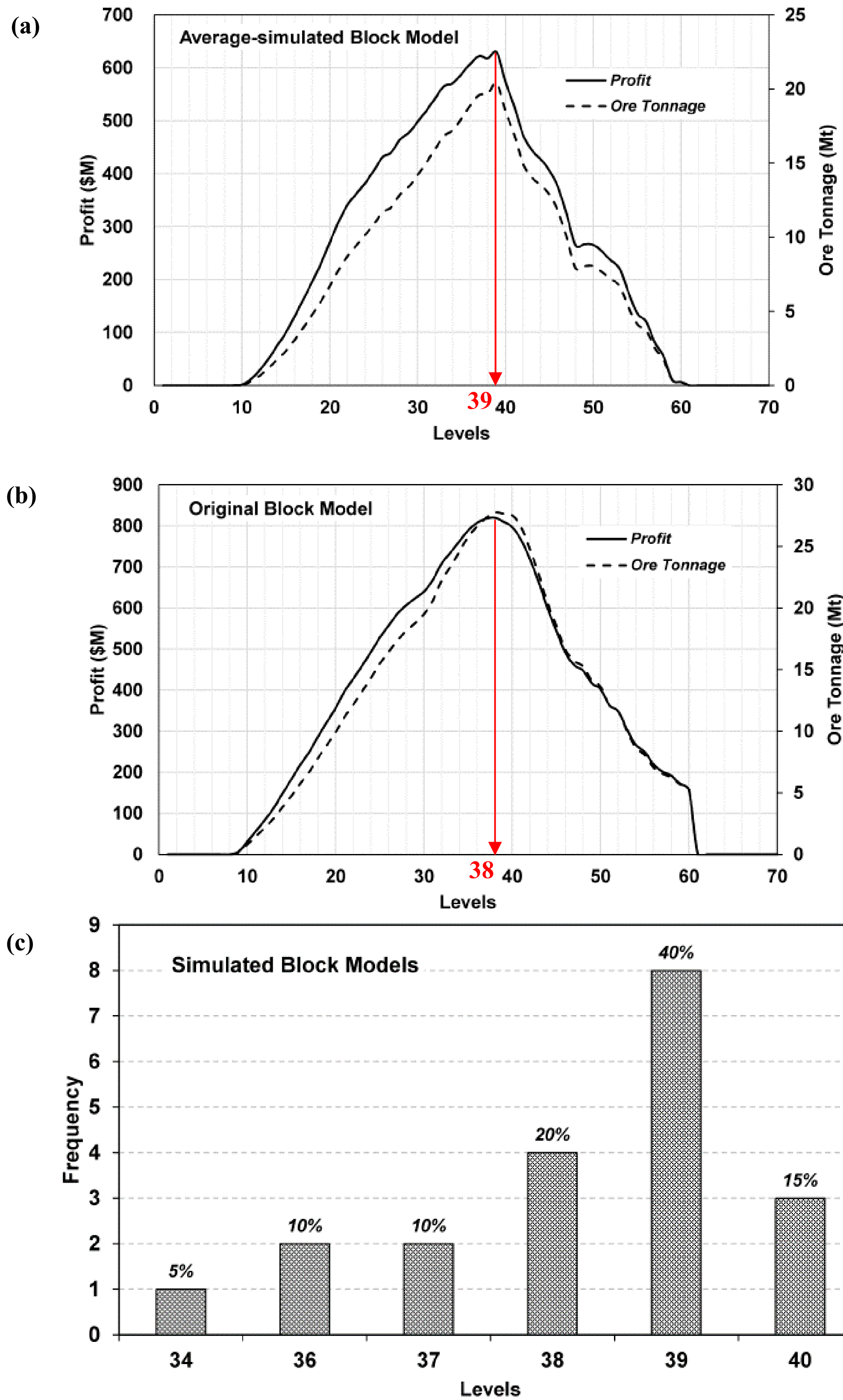

Fig 10. (a) Best level selection based on tonnage-profit curve of average-simulated block model, (b) best level selection based on tonnage-profit curve of original block model, (c) histogram of best level of extraction for simulations

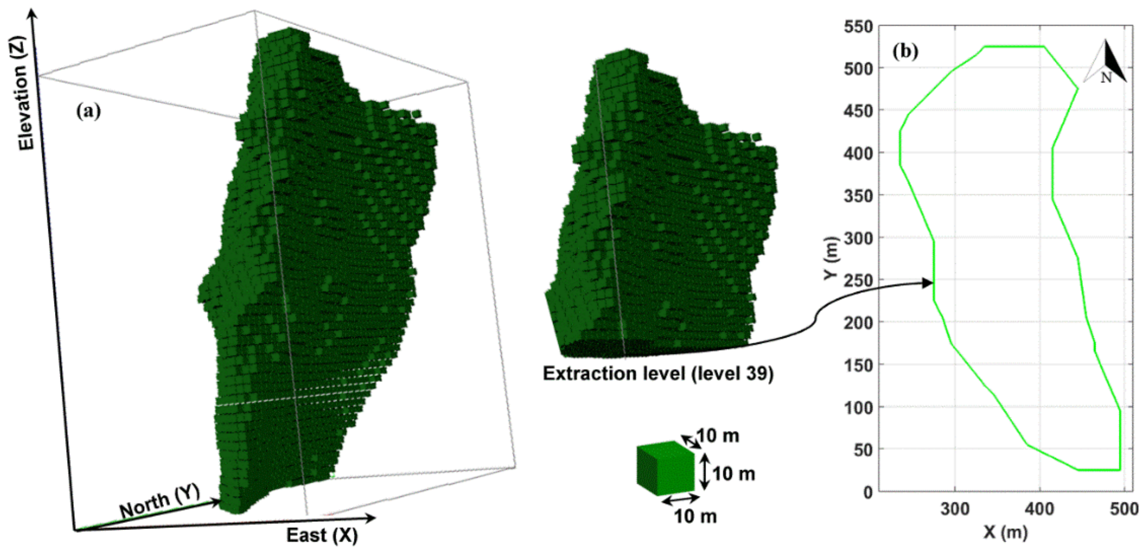

Fig 11. (a) Block model of ore-body, (b) outline of ore-body at level 39

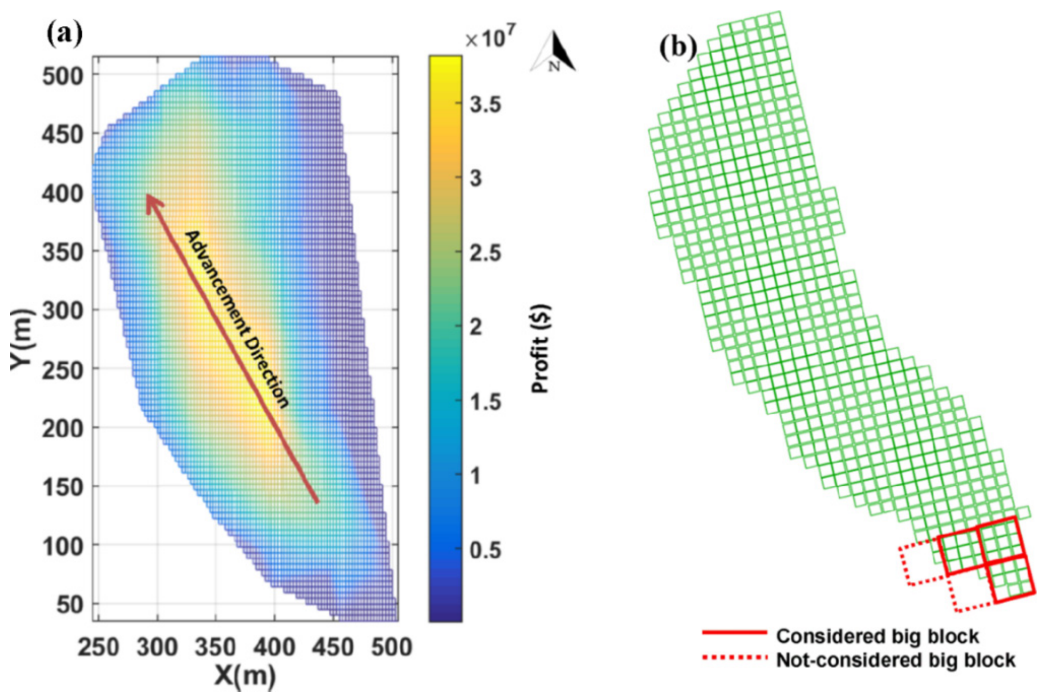

Fig 12. (a) Best advancement Direction based on the profit at the best level, (b) Schematic view of considering big-blocks with more than seven small blocks

A big-block contains seven, eight, or nine small ore blocks and all the small ore blocks above the big-block in the extraction level. Afterwards, the average grade of new big-blocks column was calculated using a weighted average method. Also, the total ore tonnage and profit values of each big-block column were calculated. After the big-block columns were created, the optimal production schedule was generated for the columns. The objective was to maximize the NPV. Table 3 shows the scheduling parameters to generate the production schedule. The coefficient matrices were created in MATLAB (Math Works Inc., 2015). CPLEX (IBM, 2015) was used to solve the problem. The model was run for level 39 on original block model with 91 big-block columns over 15 periods.

Table 3. Scheduling parameters

Parameter	Value	Parameter	Value
T	15	$P(\$/tonne)$	6,000
$MCL\ (Mt)$	1.2	$SC\ (\$/tonne)$	0.5
$MCU\ (Mt)$	3	$MC\ (\$/tonne)$	10
$GL(\%)$	1.3	$PC\ (\$/tonne)$	16.1
$GU(\%)$	1.6	$\overline{N}_{NBBL,1}$	27
$ExtL\ (Mt)$	0.09	$\underline{N}_{NBBL,1}$	0
$ExtU\ (Mt)$	0.35	$\overline{N}_{NBBL,t}$	5
$i(\%)$	10	$\underline{N}_{NBBL,t}$	2
$R(\%)$	85		

The amount of extracted ore was 39 Mt with the NPV of $1.036 B. Fig 13 shows the production average grade and production tonnage in each period for this level. As it can be seen from the production graph, the maximum amount of material has been extracted in early periods and for the rest of the mine life it has been decreased gradually. Also in the grade graph, it has been increased slowly in early periods and the material with higher grades were extracted at first, then it starts decreasing near the end of the mine life. Fig 14 shows the number of active and new big-blocks in which the number of new big-blocks are within the defined range. The formulation tries to open more big-blocks at the first period in order to maximize the NPV and because of that 25 big-blocks were opened at period one. Moreover, the precedence of extraction is shown in Fig 15.

The tonnage and NPV changes for all the realizations and original block model at level 39 were examined. Fig 16 illustrates the frequency of NPV at level 39 for all the realizations. As it can be seen, the NPV varies between $0.96 B and $1.08 B. Fig 17 shows the tonnage analysis, the ore tonnage changes between 33.1 Mt and 39.6 Mt and for the original block model it stands above the average.

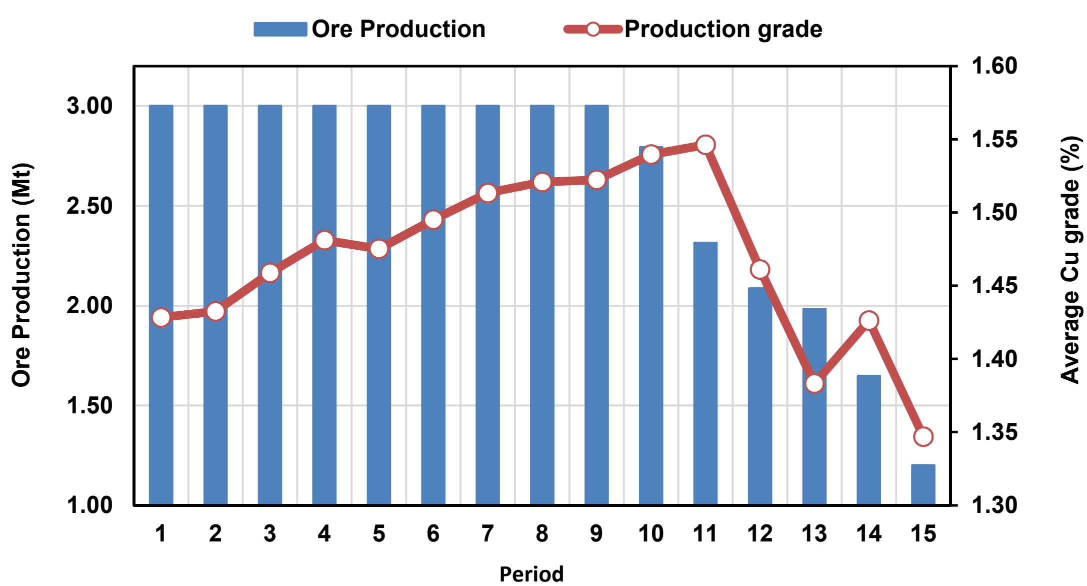

Fig 13. Production tonnage and average grade of production at level 39

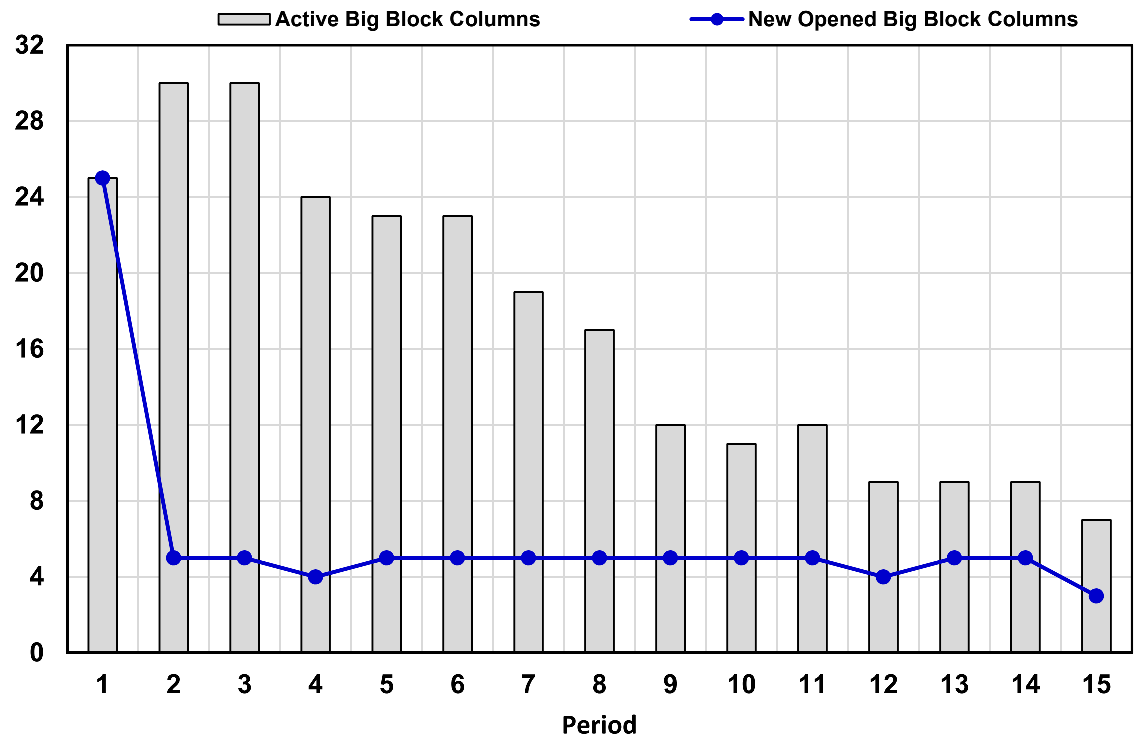

Fig 14. Number of active and new big-blocks for each period at level 39

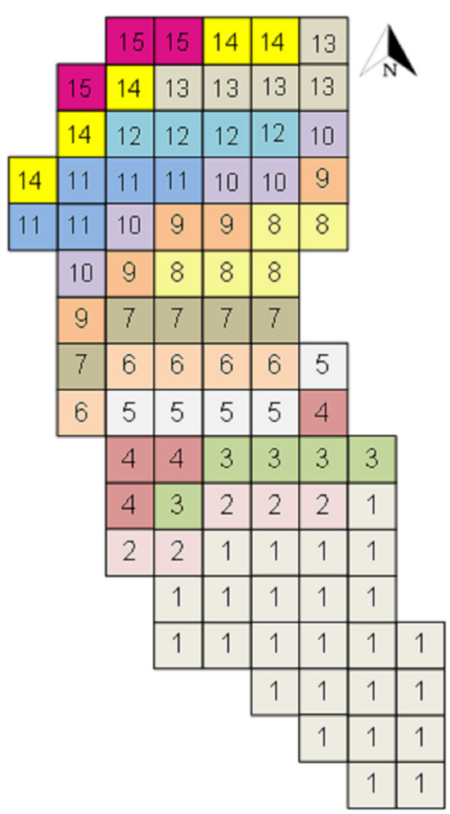

Fig 15. Starting extraction period of big-blocks at level 39 (numbers represent the starting period)

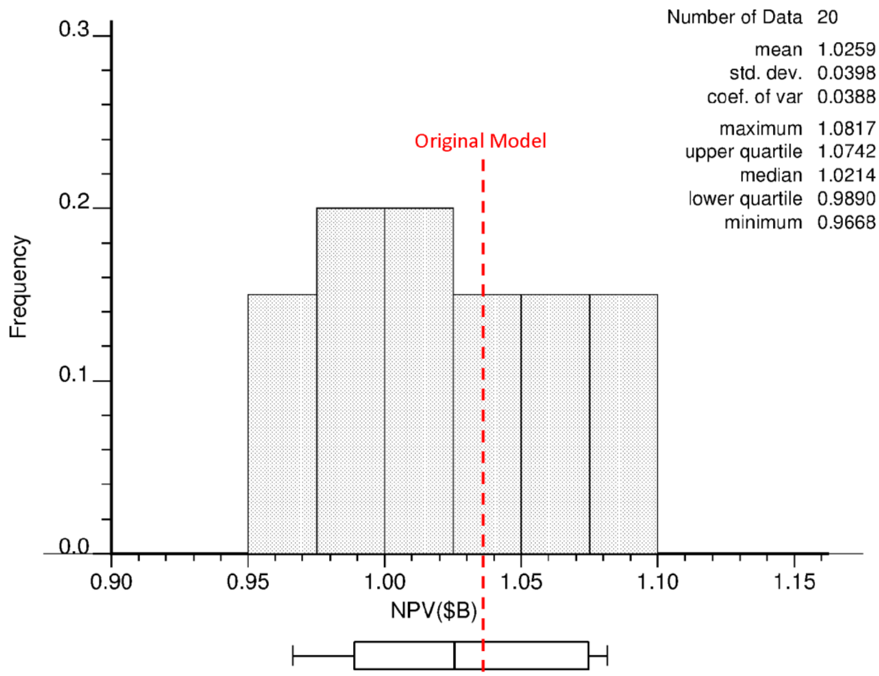

Fig 16. The NPV frequency for all the realizations at level 39

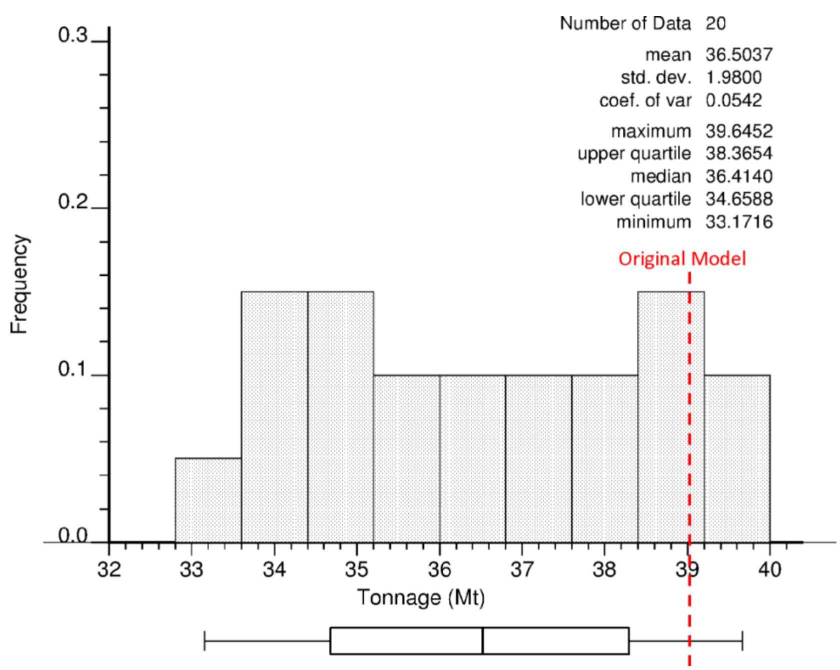

Fig 17. The tonnage frequency for all the realizations at level 39

6. Conclusion

Geological uncertainty has been used in open-pit mining, but is less studied in underground mining, especially in block caving, where it is not so easy to revise production plans after caving has begun. The methodology used in this paper is able to find the best extraction horizon placement under grade uncertainty. Also, it is able to define an optimal production scheduling using mathematical programming and MILP formulation in MATLAB and solving it using CPLEX.

Optimizing one block model (original or average-simulated) will result in a single number. But when a number of block models are optimized, the obtained results show a range associated with the risk of project.

The results from the NPV analysis showed that the difference between the NPV of original block model and the minimum value was 7.15% and the difference from the maximum value was 4.41%. Following the same manner for tonnage, those differences from minimum and maximum values were 17.63% and 1.6%, respectively.

7. References

[1] Albor, F. and Dimitrakopoulos, R. (2009). Stochastic mine design optimization based on simulated annealing: pit limits, production schedules, multiple orebody scebarios and sensitivity analysis. *IMM Transactions Mining Technology*, *118* (2), 80-91.

[2] Alonso-Ayuso, A., Carvallo, F., Escudero, L. F., Guignard, M., Pi, J., Puranmalka, R., and Weintraub, A. (2014). Medium range optimization of copper extraction planning under uncertainty in future copper prices. *European Journal of Operational Research*, *233* (3), 711-726.

[3] Asad, M. W. A. and Dimitrakopoulos, R. (2013). Implementing a parametric maximum flow algorithm for optimal open pit mine design under uncertain supply and demand. *Journal of the Operational Research Society*, *64* (2), 185-197.

[4] Carpentier, S., Gamache, M., and Dimitrakopoulos, R. (2016). Underground long-term mine production scheduling with integrated geological risk management. *Mining Technology*, *125* (2), 93-102.

[5] Chanda, E. C. K. (1990). An application of integer programming and simulation to production planning for a stratiform ore body. *Mining Science and Technology*, *11* (2), 165-172.

[6] Deutsch, C. V. and Journel, A. G. (1998). *GSLIB : geostatistical software library and user's guide.* Vol. 2, Oxford University Press, New York,369.

[7] Diering, T. (2004). *Computational considerations for production scheduling of block cave mines*. in Proceedings of MassMin 2004, Santiago, Chile, pp. 135-140.

[8] Diering, T. (2012). Quadratic Programming applications to block cave scheduling and cave management. in *Massmin 2012*. Sudbury, Canada, pp. 1-8.

[9] Diering, T., Richter, O., and Villa, D. (2008). Block cave production scheduling using PCBC. in *MassMin 2008*. Luleå, Sweden.

[10] Dimitrakopoulos, R. and Ramazan, S. (2008). Stochastic integer programming for optimising long term production schedules of open pit mines: methods, application and value of stochastic solutions. *Mining Technology*, *117* (4), 155-160.

[11] Dowd, P. A. (1994). Risk assessment in reserve estimation and open-pit planning. *Trans. Instn. Min. Metall.*, *103* A148 - A154.

[12] Epstein, R., Goic, M., Weintraub, A., Catalán, J., Santibáñez, P., Urrutia, R., Cancino, R., Gaete, S., Aguayo, A., and Caro, F. (2012). Optimizing Long-Term Production Plans in Underground and Open-Pit Copper Mines. *Operations Research*, *60* (1), 4-17.

[13] Grieco, N. and Dimitrakopoulos, R. (2007). Managing grade risk stope design optimisation: Probabilistic mathematical programming model and application in sublevel stoping. *IMM Transactions Mining Technology*, *116* (2), 49-57.

[14] Guest, A. R., Van Hout, G. J., and Von Johannides, A. (2000). *An Application of Linear Programming for Block Cave Draw Control*. in Proceedings of MassMin, The Australasian Institute of Mining and Metallurgy, Brisbane, Australia, pp. 461-468.

[15] IBM (2015). IBM ILOG CPLEX 12.6.2. Ver.

[16] Khodayari, F. and Pourrahimian, Y. (2014). Determination of the best height of draw in block cave sequence optimization. in *Mass Min 2014*. Santiago, Chile, pp. 457-465.

[17] Khodayari, F. and Pourrahimian, Y. (2015). Determination of development precedence for drawpoints in block-cave mining. in *5th International Symposium Mineral Resources and Mine Development (AIMS 2015)* Aachen, Germany, pp. 383-391.

[18] Koushavand, B. and Askari-Nasab, H. (2009). Transfer of Geological Uncertainty into Mine Planning. in *Mine Planning and Equipment Selection (MPES) CD-ROM*. Banff, Alberta, Canada, pp. 462-476.

[19] Lamghari, A. and Dimitrakopoulos, R. (2012). A diversified Tabu search approach for open-pit mine production scheduling problem with metal uncertainty. *European Journal of Operational Research*, *222* (3), 642-652.

[20] Lamghari, A., Dimitrakopoulos, R., and Ferland, J. (2013). A variable neighbourhood decent algorithm for the open-pit mine production scheduling problem with metal uncertainty *Journal of the Operational Research Society 65* (9), 1305-1314.

[21] Leite, A. and Dimitrakopoulos, R. (2007). Stochastic optimization model for open-pit mine planning: application and risk analysis at a copper deposit. *IMM Transactions Mining Technology*, *116* (3), 109-118.

[22] Lerchs, H. and Grossmann, I. (1965). Optimum design of open-pit mines. *Canadian Mining Metallurgical Bull*, *58* 17-24.

[23] Maleki, M. and Emery, X. (2015). Joint simulation of grade and rock type in a stratabound copper deposit *Mathematical Geosciences 47* (4), 471-495.

[24] Montiel, L., Dimitrakopoulos, R., and Kawahata, K. (2015). Globally optimising open-pit and underground mining operations under geological uncertainty. *Mining Technology*, *00* (0), 1-13.

[25] Osanloo, M., Gholamnejad, J., and Karimi, B. (2008). Long-term open pit mine production planning: a review of models and algorithms. *International Journal of Mining, Reclamation and Environment*, *22* (1), 3-35.

[26] Parkinson, A. (2012). Essays on Sequence Optimization in Block Cave Mining and Inventory Policies with Two Delivery Sizes.Thesis, The University Of British Columbia, The University Of British Columbia, Pages 199.

[27] Pourrahimian, Y. and Askari-Nasab, H. (2014). An application of mathematical programming to determine the best height of draw in block-cave sequence optimization. *Mining Technology (Trans. Inst. Min. Metall. A)*, *123* (3), 162-172.

[28] Pourrahimian, Y., Askari-Nasab, H., and Tannant, D. (2013). A multi-step approach for block-cave production scheduling optimization. *International Journal of Mining Science and Technology*, *23* (5), 739-750.

[29] Rahal, D., Dudley, J., and Hout, G. v. (2008). *Developing an optimised production forecast at Northparkes E48 mine using MILP*. in Proceedings of 5th International Conference and Exhibition on Mass Mining, Luleå Sweden, pp. 227-236.

[30] Ramazan, S. and Dimitrakopoulos, R. (2004). Traditional and New MIP Models for Production Scheduling With In-Situ Grade Variability. *International Journal of Surface Mining, Reclamation and Environment*, *18* (2), 85-98.

[31] Ramazan, S. and Dimitrakopoulos, R. (2013). Production scheduling with uncertain supply: a new solution to the open-pit mining problem *Optimization and Engineering*, *14* (2), 361-380.

[32] Ravenscroft, P. (1992). Risk analysis for mine scheduling by conditional simulation. *Canadian Mining and Metallurgical Bulletin*,

[33] Rubio, E. (2002). Long term planning of block caving operations using mathematical programming tools.Thesis, The University of British Columbia, Pages 126.

[34] Rubio, E. and Diering, T. (2004). *block cave production planning using operation research tool*. in Proceedings of Massmin 2004, Gemcom, Santiago, Chile, pp. 141-149.

[35] Sabour, S. A. and Dimitrakopoulos, R. (2011). Incorporating geological and market uncertainties and operational flexibility into open pit mine design. *Journal of Mining Science*, *47* (2), 191-201.

[36] Smoljanovic, M., Rubio, E., and Morales, N. (2011). *Panel Caving Scheduling Under Precedence Constraints Considering Mining System*. in Proceedings of 35th APCOM Symposium, Wollongong, NSW, Australia, pp. 407-417.

[37] Song, X. (1989). *Caving process simulation and optimal mining sequence at Tong Kuang Yu mine, China*. in Proceedings of pp. 386-392.

[38] Vargas, E., Morales, N., and Emery, X. (2014). *Footprint and economic envelope calculation for block/panel caving mines under geological uncertainty*. in Proceedings of Caving 2014, Santiago, Chile, pp. 449-456.

[39] Weintraub, A., Pereira, M., and Schultz, X. (2008). A Priori and A Posteriori Aggregation Procedures to Reduce Model Size in MIP Mine Planning Models. *Electronic Notes in Discrete Mathematics 30* 297–302.